

Reverse Monte Carlo analysis for small-angle scattering of expanded fluid Hg: connection to the wide-angle structure factor

K. Hagita,^{a*} T. Arai,^a M. Inui,^b K. Matsuda^c and K. Tamura^c

^aDepartment of Applied Physics, National Defense Academy, Yokosuka 239-8686, Japan, ^bFaculty of Integrated Arts and Sciences, Hiroshima University, Higashi-Hiroshima 739-8521, Japan, and ^cFaculty of Engineering, Kyoto University, Kyoto 606-8501, Japan. Correspondence e-mail: hagita@nda.ac.jp

A preliminary result of reverse Monte Carlo (RMC) analysis of small-angle X-ray scattering data for expanded fluid Hg with the help of wide-angle X-ray diffraction data in the same thermodynamic state is presented. In RMC analysis, three-dimensional configurations of 100000 Hg atoms were modeled to see the large density fluctuation associated with liquid–vapor critical phenomena. It was found that interpolation of measured structure factors is necessary for RMC analysis.

© 2007 International Union of Crystallography
Printed in Singapore – all rights reserved

1. Introduction

Liquid Hg expanded along the vapor–liquid coexistence curve undergoes a metal–non-metal transition at a density of about 9 g cm^{-3} and at a critical point of around 6 g cm^{-3} . Near the critical point, large density fluctuations cause increasing structure factors in small-angle regions.

A series of energy-dispersive X-ray diffraction (XRD) measurements for expanded fluid Hg up to the supercritical region have been carried out using synchrotron radiation at SPring-8 (Inui *et al.*, 2003). They have provided structure factors covering a sufficiently wide range of the modulus of the scattering vector, $q > 1 \text{ \AA}^{-1}$ ($q = 4\pi E \sin\theta/hc$, where θ is half of the scattering angle, h is Planck's constant, c is the velocity of light and E is the X-ray energy).

In previous papers (Arai & McGreevy, 1998; Inui *et al.*, 2003), we discovered that three different regions of density exist in fluid Hg from the liquid to the dense vapor state and that fluid Hg contains atoms which can be considered as being a 'metallic' environment, characterized by a larger number of nearest neighbors at a relatively short distance, and atoms which are in a 'semiconducting' environment, characterized by a smaller number of neighbors at a slightly greater distance. These ideas are based on a detailed analysis of structure factors obtained from wide-angle XRD data and can explain changes in the local structure of expanded fluid Hg.

Recently Inui, Matsuda & Tamura (unpublished) have carried out small-angle X-ray scattering (SAXS) measurements for expanded fluid Hg in the same thermodynamic states as the XRD data. They have obtained structure factors for q ranging from 0.04 to 0.36 \AA^{-1} . In order to estimate the absolute SAXS intensity of expanded fluid Hg, $I(q)$, the scaling factor is obtained from the measurements of compressed He gas. We subtracted the background intensity of compressed He gas from the observed spectra of fluid Hg after it had been scaled for sample transmission. Subsequently, the SAXS intensity of fluid Hg was normalized with the scaling factor and $S(q)$ was deduced from

$$S(q) = \frac{I(q)}{Nf^2(q)}, \quad (1)$$

where N is the number of atoms and $f(q)$ is the atomic form factor. These experiments reveal that a quite large density fluctuation exists in expanded fluid Hg near the critical region. Many interesting questions arise from the results. First, how does the large density fluctuation correlate with the local structure, the distribution of the coordination numbers and/or the inter-atomic distances? Second, how are the sizes of the fluctuation in real space distributed? In addition, seeing the structural changes from the liquid side to the gas side near the critical point in real space will greatly contribute to insight into the critical phenomena.

Reverse Monte Carlo (RMC) analysis that can provide three-dimensional atomic configurations from observed scattering data has been proven to be a powerful tool for studying the structure of disordered materials (McGreevy & Pusztai, 1988; Arai & McGreevy, 1998; McGreevy, 2001) and may be expected to answer the important questions above.

In the past ten years of RMC analysis, the experimental data of SAXS have not been examined in detail because the required system size in constructing a model is huge.

Recently, Pusztai *et al.* (2004) have performed RMC modeling on the structure of colloidal aggregates by using the artificial structure factor in a wide q -space region including a small-angle region. The structure factor as an experimental datum, which is the input datum for RMC analysis, is calculated from the three-dimensional configuration made by a computer simulation for diffusion-limited cluster aggregation (DLCA). In order to study a large system such as a colloidal aggregation, the particles in this RMC analysis correspond to the aggregated clusters of atoms (coarse-grained atoms) instead of to the single atom used in conventional RMC analysis. They confirmed that the fractal dimension of the configuration estimated by RMC analysis, using the number densities $\rho = 0.05\text{--}0.1$ and the number of particles $N = 6250\text{--}12500$, is consistent with that of the original DLCA configuration.

Very recently, the RMC method has been extended for the analysis of two-dimensional patterns of the structure factor of uni-axial systems (Hagita *et al.*, 2006). This extended RMC analysis is used for the modeling of a three-dimensional configuration from the structure factor by two-dimensional ultra-small-angle X-ray scattering experi-

ments of the silica particles in uni-axially elongated rubbers (Shinohara *et al.*, 2005).

This result suggests that RMC analysis is available for small-angle scattering data if the corresponding structure factor is correctly extracted from the scattering data.

In this paper, we present a preliminary result of RMC analysis of SAXS data for expanded fluid Hg with the help of wide-angle X-ray diffraction (XRD) data (Inui *et al.*, 2003) in the same thermodynamic state. The typical experimental data for both experiments are shown in Fig. 1. Here, we have no scaling treatment for plotting both data sets. Unfortunately we do not have structure factor data in the intermediate range ($q = 0.36\text{--}1.36 \text{ \AA}^{-1}$). It is also interesting to see whether RMC analysis can provide physically correct structure factor data in the intermediate region in expanded fluid Hg.

In §2, reverse Monte Carlo analysis is briefly explained and modifications used in this work are presented. In §3, the results of RMC analysis for expanded fluid Hg around its critical points are presented. The validity of obtained interpolated data for structure factors among SAXS and XRD is examined. A summary and discussion are given in the last section.

2. Reverse Monte Carlo analysis

RMC analysis is widely used as a general method for diffraction data analysis for disordered materials (McGreevy, 2001). The details of the method have been described in early works (McGreevy & Pusztai, 1988; McGreevy, 1992). It can model three-dimensional structures in a real space, that is, atomic configurations from a measured structure factor $S^{\text{exp}}(q)$. Actually it iteratively replaces the atomic configuration so that the difference between observed and calculated structure factors is minimized within the errors. In general, a structure factor is defined from an atomic configuration in the following equation

$$S(q) = \frac{1}{N} \sum_{i,j=1}^N \exp[-i\mathbf{q} \cdot (\mathbf{r}_i - \mathbf{r}_j)], \quad (2)$$

where N denotes number of atoms in the system, \mathbf{r}_i the position of the i -th atom and \mathbf{q} the scattering vector. We briefly summarize the simulation procedure in the following steps:

(i) A simulation starts with the initial configuration of atoms set in a box under the periodic boundary condition. The size of the box is determined by the measured density for $S^{\text{exp}}(q)$. Usually the initial

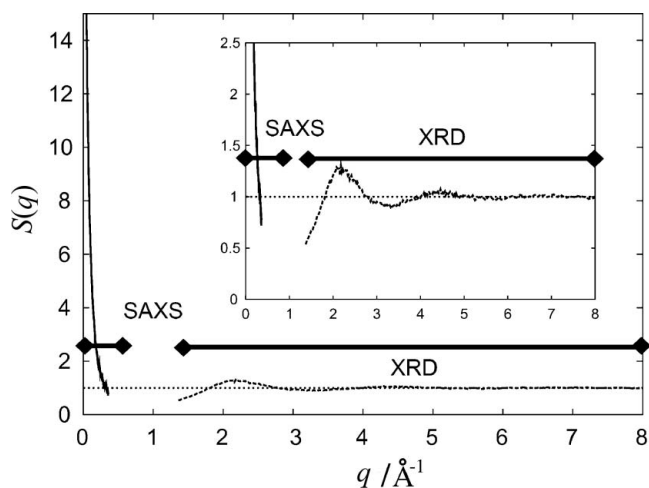


Figure 1
Structure factor of fluid Hg measured by SAXS and XRD at $T = 1840 \text{ K}$ and $\rho = 5.07 \text{ g cm}^{-3}$.

configuration is presented as a well known crystal structure or a random packing structure.

(ii) An atom and a displacement vector of a trial movement are chosen randomly, where the vector is satisfied with some physical constrains such as a volume exclusion of atoms.

(iii) First a radial distribution function $g(r)$ is calculated from the atomic configuration. Then the corresponding $S^{\text{comp}}(q)$ are calculated by Fourier transformation of $g(r)$ instead of equation (2). The difference $\Delta(\chi^2)$ of the goodness-of-fit parameter χ^2 in each move is calculated, where

$$\chi^2 = \sum_q \frac{[S^{\text{exp}}(q) - S^{\text{comp}}(q)]^2}{\sigma^2} \quad (3)$$

and σ is the standard deviation.

(iv) For $\Delta(\chi^2) \leq 0$, every trial move is accepted. Trial moves which worsen the fit [$\Delta(\chi^2) > 0$] are accepted with a probability, $P = \exp[-\Delta(\chi^2)/2]$.

(v) The sequences from step (ii) to step (iv) are repeated until χ^2 converges.

In order to perform RMC analysis for SAXS data, which requires a larger number of atoms, we have modified the programming code (RMCA version 3.04), which is widely used.¹ The most significant points of these modifications are as follows: a parallelized programming technique using OpenMP (Open Multi Processing) is applied in order to shorten the execution time. The algorithm for the calculation of χ^2 is extended for the error-bars [standard deviation $\sigma(q)$] so that it depends on the value of q . It is expected that the error-bars of the structure factor for large-scale features are relatively larger than those for small-scale features because of the statistics. Equation (3) is rewritten as follows

$$\chi^2 = \sum_q \frac{[S^{\text{exp}}(q) - S^{\text{comp}}(q)]^2}{\sigma^2(q)}. \quad (4)$$

We use data points with q from 0.04 to 0.36 \AA^{-1} for SAXS and 1.36 to 8.0 \AA^{-1} for XRD, which are shown in Fig. 1. Despite the absence of measured data, RMC can fit both $S(q)$ s. This is the first result of the RMC analysis for the connection between SAXS and XRD measurements. However there is no guarantee that the estimated structure factor between SAXS and XRD measurements is correct. Besides the analysis for such discontinuous $S(q)$ by SAXS and XRD, we also examine $S(q)$ with some interpolated data which are obtained from both sets of experimental data.

We choose about 200 \AA as the size of the simulation box for producing $S(q)$ in a small-angle range. As a result, the number of Hg atoms becomes a sub-mega (10^5) order. In the RMC procedure, the values of the standard deviation σ and cutoff are changed in order to enhance the relaxation process from the initial positions. In the final stage of the RMC procedure, we use the following parameter: standard deviation $\sigma = 0.002$, cutoff $r_c = 2.3 \text{ \AA}$ and spacing of a grid $\Delta r = 0.05 \text{ \AA}$.

¹The programming code of RMCA (version 3.04) had been distributed by Studsvik Neutron Research Laboratory. The web site of this laboratory is closed. However, the code can be obtained from the web site of CCP14 (Collaborative Computational Project number 14) at the present time. A recent version of program for the Windows OS is distributed at the renewed web site (<http://www.isis.rl.ac.uk/RMC>) in ISIS.

Table 1

Values of density ρ , temperature T and pressure P around the critical point.

Calculated values of number density and size L of the box by periodic boundary condition are also given.

ρ (g cm ⁻³)	T (K)	P (bar)	Number density (\AA^{-3})	L (\AA)
10.1	1773	1750	0.03032	148.9
9.62	1673	1917	0.02888	151.3
5.70	1840	1930	0.01711	181.3
4.09	1818	1760	0.01228	201.2
3.06	1818	1610	0.009186	221.6

3. Results

3.1. Analysis with absent data

Inui, Matsuda and Tamura have carried out SAXS measurements of expanded fluid Hg in 15 distinct thermodynamic states, which are the same states as those for the XRD data. We employ some of them around the critical point in the present work. The values of density, temperature and pressure used are listed in Table 1.

For all cases, after about 10^6 acceptance moves, atomic configurations do not significantly change any more. Some of them appear not to be in convergence at high q . We ignore the fine differences in this case.

Fig. 2 shows the resulting structure factor [$S^{\text{exp}}(q)$ and $S^{\text{comp}}(q)$] of expanded fluid Hg with higher density than the critical density. The

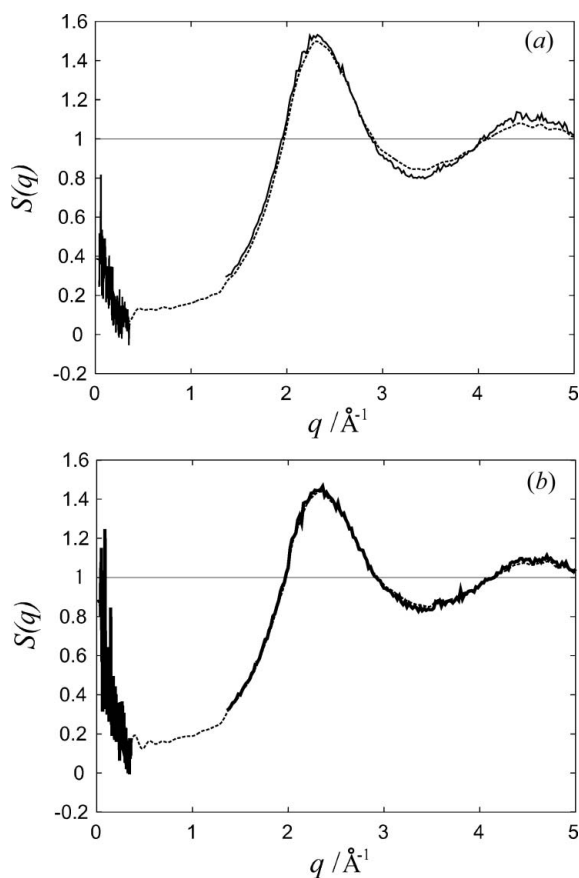


Figure 2
Structure factors of fluid Hg produced using SAXS and XRD at (a) $T = 1773$ K and $\rho = 10.1$ g cm⁻³ and (b) $T = 1673$ K and $\rho = 9.62$ g cm⁻³. The solid lines denote the experimental data and the dashed lines denote the obtained $S(q)$.

detailed thermodynamics are listed in the figure caption and Table 1. Although the data for SAXS have larger errors than for wide-angle XRD data, RMC seems to reasonably connect both data except a few points close to the experimental data.

Fig. 3 shows the resulting structure factor [$S^{\text{exp}}(q)$ and $S^{\text{comp}}(q)$] of expanded fluid Hg with lower density than the critical density. In comparison with Fig. 2, the contribution to the value of $S(q)$ from SAXS become large. Although the data for SAXS have smaller errors than those in Fig. 2, RMC provides strange structure factors for the connection between the lower wavenumber region for SAXS data and the higher wavenumber region for XRD data.

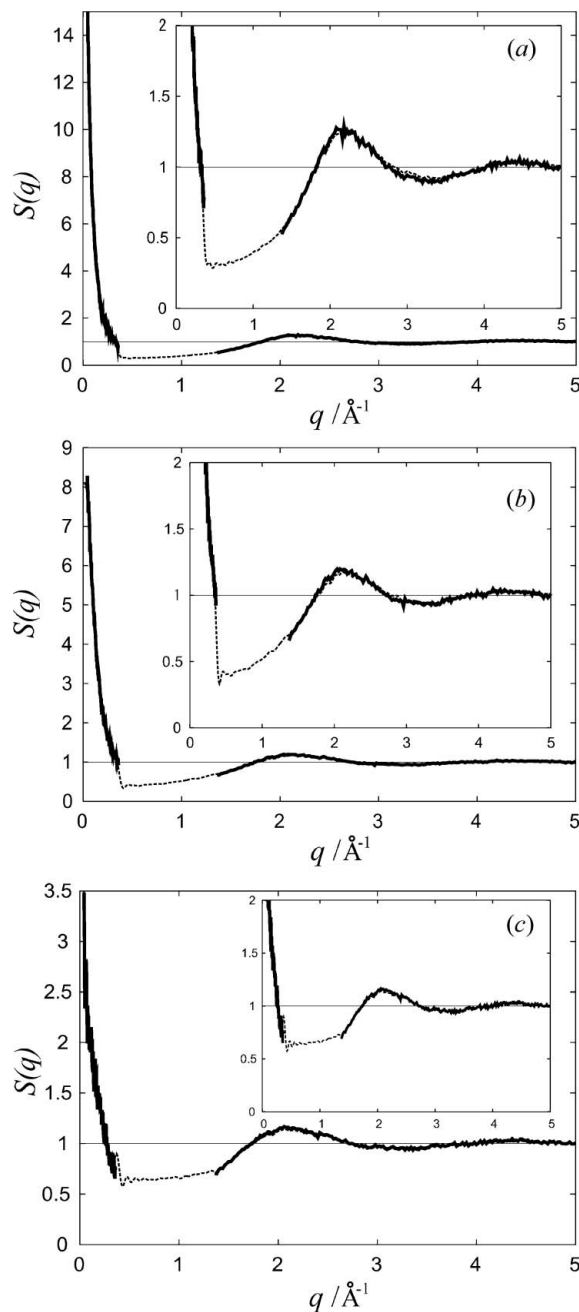


Figure 3
Structure factors of fluid Hg produced by SAXS and XRD at (a) $T = 1840$ K and $\rho = 5.70$ g cm⁻³, (b) $T = 1818$ K and $\rho = 4.09$ g cm⁻³ and (c) $T = 1818$ K and $\rho = 3.06$ g cm⁻³. The inset shows the magnification around $S(q) = 1$. The solid lines denote the experimental data and the dashed lines denote the obtained $S(q)$.

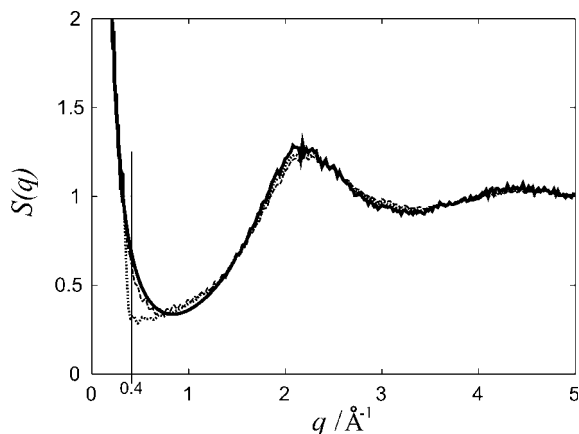


Figure 4 RMC results using $S^{\text{approx}}(q)$ and $S(q)$ without it. The solid line denotes $S^{\text{exp}}(q)$ including $S^{\text{approx}}(q)$, the dashed line denotes $S^{\text{comp}}(q)$ by RMC and the dotted line denotes the same $S^{\text{comp}}(q)$ in Fig. 3(a).

In these RMC analyses, the choice (pathway) of parameters is important for obtaining results with a good fit. Indeed we have done it in the following way.

(i) Firstly, rough fitting of RMC analysis was performed. The obtained structure factor for the wide-angle region was not in agreement with the experimental data.

(ii) In order to improve the fit of the structure factor for the wide-angle region, we performed RMC analysis by using the structure factor only for the wide-angle region ($1.36 < q < 8.0 \text{ \AA}^{-1}$).

(iii) Finally, RMC analysis with the all experimental data was performed again.

We consider that the pathway of parameters is independent of the final result because the changing of the parameters contributes only to the acceleration of the relaxation of the initial configuration.

It is considered that the standard deviations $\sigma(q)$ in $S(q)$ for large scale features, that is, in $q < 0.36 \text{ \AA}^{-1}$ are relatively larger than those for small scale features because of the statistics. We examine the case that the standard deviation $\sigma(q) = 0.2$ for SAXS data are set to 100 times larger than $\sigma(q) = 0.002$ for XRD data. We can obtain good results in a shorter execution time than the case with a uniform standard deviation $\sigma = 0.002$. The obtained result was in good agreement with the result shown in Figs. 2 and 3. (The result is not shown in a figure because the difference is negligibly small.) It is expected that the time to convergence in the case using the well suited error-bars $\sigma(q)$ becomes shortest. We believe that such a well suited error size can be obtained from the experiments. The RMC analysis with suitable error size $\sigma(q)$ should be performed in the future.

3.2. Analysis with interpolated data

According to the theory on the structure of liquid in the liquid-vapor critical region (March, 1990 and references therein), The critical behavior of the structure factor is approximately expressed by $S(q) \sim \text{Const}/q^{2-\eta}$; $T = T_c$, $q \rightarrow 0$, where η is some critical exponent and small value for real liquids. In the Ornstein-Zernike treatment, $\eta = 0$. It is not certain that this approximation is valid for the case of expanded fluid Hg. Therefore we will extrapolate the SAXS data to the region of the absent structure factor by making the above assumption and also extrapolate the XRD data to the same region by using a function determined *ad hoc*. In the present study we have an hypothesis that $S(q)$ for $q < 1.5 \text{ \AA}^{-1}$ is approximated by a function

described by two exponents: $S^{\text{approx}}(q) = C_1 q^\alpha + C_2 q^\beta$. We interpolated $S(q)$ for the case $T = 1840 \text{ K}$ and $\rho = 5.70 \text{ g cm}^{-3}$, the parameter set $C_1 = 0.15$, $\alpha = -1.66$, $C_2 = 0.2$ and $\beta = 2.5$ gives good fit with the experimental data. The value for α was close to -2.0 . This result is shown in Fig. 4. Fig. 4 shows that RMC result using continuous $S(q)$ with the interpolated data is different around $q = 0.5 \text{ \AA}^{-1}$ from the results in Fig. 3(a). We think this result is better than the result in Fig. 3.

It suggests that $S(q)$ for $0.4 < q < 0.6 \text{ \AA}^{-1}$ is very important for the reliable RMC analysis. However it seems to be very difficult to measure the structure factor in this region because of the low intensity of the scattering.

3.3. Visualization of fluctuations

In order to gain a physical insight of the large density fluctuations of expanded fluid Hg around the critical point, the first thing to do is the visualization of the large density fluctuations. A snap-shot of one of the obtained three-dimensional configurations by RMC for the case $T = 1840 \text{ K}$ and $\rho = 5.70 \text{ g cm}^{-3}$ is shown in Fig. 5. We can not find any clear pattern related to the large density fluctuations in this picture. For emphasizing these large density fluctuations, we have

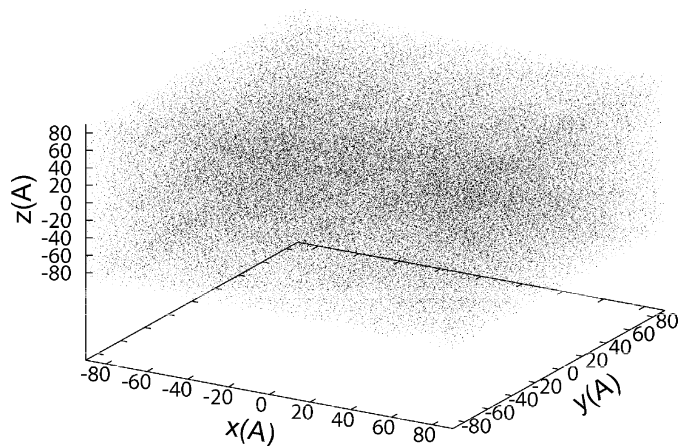


Figure 5 Snap-shot of the three-dimensional configuration obtained by RMC analysis for the case $T = 1840 \text{ K}$ and $\rho = 5.70 \text{ g cm}^{-3}$. About 100000 atoms are drawn by points. The unit for the axes is \AA .

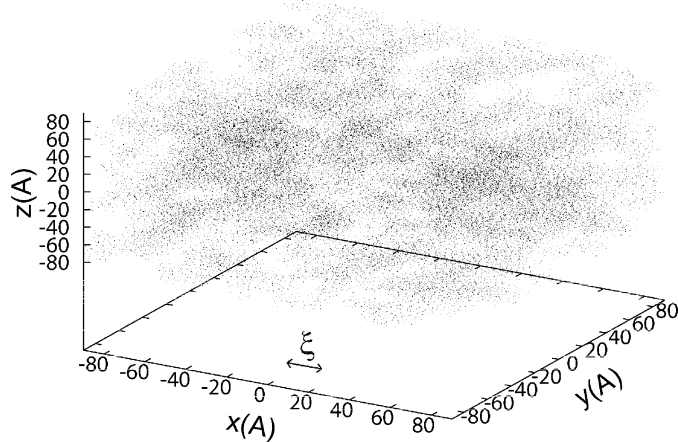


Figure 6 Modified snap-shot of the three dimensional configuration obtained by RMC analysis for the case $T = 1840 \text{ K}$ and $\rho = 5.70 \text{ g cm}^{-3}$. ξ represents the estimated correlation length.

taken an average of the local density of the configuration in the following way.

(i) The space under the periodic boundary condition is divided into $16^3 = 4096$ cubic cells.

(ii) The particles which belong to cells and whose density is below 1.1 times the average density, are removed.

Fig. 6 shows a typical snap-shot obtained from the above average treatments. Inui, Matsuda & Tamura have estimated the correlation lengths ξ for all their SAXS data using Ornstein–Zernike fitting. The corresponding value ξ of the data for Fig. 6 is estimated to be 17.1 Å, which is indicated in the figure.

At the present time, we can not derive a meaningful insight from the picture in Fig. 6. The physical consideration and interpretation of this averaging treatment will make a contribution to studies on phenomena observed using SAXS.

4. Summary

The preliminary results of reverse Monte Carlo analysis for the data from small-angle scattering for expanded Hg are presented. We model the three-dimensional configuration of about 100000 atoms at some thermodynamic states of expanded fluid Hg around the critical point. However, to obtain a reliable configuration, it is necessary to interpolate the measured data given by SAXS (from 0.04 to 0.36 \AA^{-1}) and XRD (from 1.36 to 8.0 \AA^{-1}). If possible, precise structure factor data in the region $q = 0.4\text{--}1.5 \text{ \AA}^{-1}$ are necessary and structure factor data in $q = 0.4\text{--}0.6 \text{ \AA}^{-1}$ are especially important for expanded fluid Hg. RMC analysis can visualize the large density fluctuations of expanded fluid Hg appearing near the critical point. It is confirmed that RMC analysis is a powerful tool to discuss local structures such as the distribution of the coordination number and/or the interatomic distances. It has also been found that the error-bars of structure factors are important in performing RMC analysis of large systems. A study in this direction is in progress.

The present work was partially supported by ‘Program for Strategic Use of Advanced Large-scale Research Facilities’ of the Ministry of Education, Culture, Sports, Science and Technology. We should acknowledge that Dr H. Suno and Dr H. Hasegawa of the Japan Agency for Marine–Earth Science and Technology (JAMSTEC) contributed to the discussions on the parallelized programming code of RMC analysis in the early stages of this work. The idea for three-dimensional plots (Figs. 5 and 6) was inspired by methods under developments for homological analysis of topological networks of particles in the collaboration between Dr T. Teramoto of the Chitose Institute of Science and Technology and one of the authors (KH), where this collaboration was partially supported by a Grant-in-Aid for Young Scientists (B) of the Ministry of Education, Culture, Sports, Science and Technology. One of the authors (KH) thanks the Information Initiative Center (Hokkaido University), the Earth Simulator Center (JAMSTEC), the Okazaki National Research Facilities (National Institutes of Natural Sciences) and the Institute for Solid State Physics (University of Tokyo) for the use of the computing facilities.

References

- Arai, T. & McGreevy, R. L. (1998). *J. Phys. Condens. Matter*, **10**, 9221–9230.
- Hagita, K., Okamoto, H., Arai, T., Kishimoto, H., Umesaki, N., Shinohara, Y. & Amemiya, Y. (2006). *AIP Conf. Proc.* **832**, 368–371.
- Inui, M., Hong, X. & Tamura, K. (2003). *Phys. Rev. B*, **68**, 094108-1-9.
- March, N. M. (1990). *Liquid Metals: Concepts and Theory*, p.103. Cambridge University Press.
- McGreevy, R. L. (1992). *Ann. Rev. Mater. Sci.* **22**, 217–242.
- McGreevy, R. L. (2001). *J. Phys. Condens. Matter*, **13**, R877–R913.
- McGreevy, R. L. & Pusztai, L. (1988). *Mol. Simul.* **1**, 359–367.
- Pusztai, L., Dominguez, H. & Pizio, O. A. (2004). *J. Colloid Interface Sci.* **277**, 327–334.
- Shinohara, Y., Kishimoto, H. & Amemiya, Y. (2005). *SPring-8 Research Frontiers 2004*, pp. 88–89.